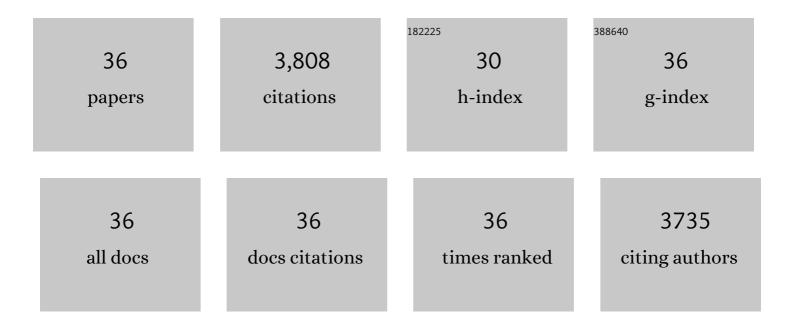


List of Publications by Year in descending order

Source: https://exaly.com/author-pdf/6521990/publications.pdf Version: 2024-02-01



LUN LI

#	Article	IF	CITATIONS
1	Self-assembled ultrathin closely bonded 2D/2D heterojunction for enhanced visible-light-induced photocatalytic oxidation and reaction mechanism insights. Journal of Colloid and Interface Science, 2022, 608, 2472-2481.	5.0	10
2	Visible-NIR light-responsive 0D/2D CQDs/Sb2WO6 nanosheets with enhanced photocatalytic degradation performance of RhB: Unveiling the dual roles of CQDs and mechanism study. Journal of Hazardous Materials, 2022, 424, 127595.	6.5	65
3	Surface reconstruction of BiSI nanorods for superb photocatalytic Cr(VI) reduction under near-infrared light irradiation. Chemical Engineering Journal, 2022, 435, 135152.	6.6	35
4	Facile assembly and excellent elimination behavior of porous BiOBr-g-C3N4 heterojunctions for organic pollutants. Environmental Research, 2022, 209, 112889.	3.7	72
5	Efficient degradation of organic pollutants by activated peroxymonosulfate over TiO2@C decorated Mg–Fe layered double oxides: Degradation pathways and mechanism. Chemosphere, 2022, 300, 134564.	4.2	35
6	Electrostatic self-assembly of 2D/2D CoWO4/g-C3N4 p—n heterojunction for improved photocatalytic hydrogen evolution: Built-in electric field modulated charge separation and mechanism unveiling. Nano Research, 2022, 15, 6987-6998.	5.8	43
7	Efficient simultaneous removal of tetracycline hydrochloride and Cr(VI) through photothermal-assisted photocatalytic-Fenton-like processes with CuOx/γ-Al2O3. Journal of Colloid and Interface Science, 2022, 622, 526-538.	5.0	12
8	Photochemical conversion of oxalic acid on heterojunction engineered FeWO4/g-C3N4 photocatalyst for high-efficient synchronous removal of organic and heavy metal pollutants. Journal of Cleaner Production, 2022, 363, 132527.	4.6	23
9	Boosting light harvesting and charge separation in 3D porous WS2@C@ZnIn2S4 skeleton heterojunction for efficient solar fuels production. Chemical Engineering Journal, 2022, 447, 137568.	6.6	29
10	Black phosphorus/Bi19Br3S27 van der Waals heterojunctions ensure the supply of activated hydrogen for effective CO2 photoreduction. Applied Catalysis B: Environmental, 2022, 317, 121727.	10.8	42
11	Van der Waals heterojunction for selective visible-light-driven photocatalytic CO2 reduction. Applied Catalysis B: Environmental, 2021, 284, 119733.	10.8	92
12	Interfacial Engineering of Bi ₁₉ Br ₃ S ₂₇ Nanowires Promotes Metallic Photocatalytic CO ₂ Reduction Activity under Near-Infrared Light Irradiation. Journal of the American Chemical Society, 2021, 143, 6551-6559.	6.6	159
13	Facile Synthesis of AgFeO ₂ â€Decorated CaCO ₃ with Enhanced Catalytic Activity in Activation of Peroxymonosulfate for Efficient Degradation of Organic Pollutants. Advanced Energy and Sustainability Research, 2021, 2, 2100038.	2.8	16
14	Optimizing electron structure of Zn-doped AgFeO2 with abundant oxygen vacancies to boost photocatalytic activity for Cr(VI) reduction and organic pollutants decomposition: DFT insights and experimental. Chemical Engineering Journal, 2021, 411, 128515.	6.6	39
15	Oxygen vacancy induced peroxymonosulfate activation by Mg-doped Fe2O3 composites for advanced oxidation of organic pollutants. Chemosphere, 2021, 279, 130482.	4.2	60
16	Synergetic effects of Bi5+ and oxygen vacancies in Bismuth(V)-rich Bi4O7 nanosheets for enhanced near-infrared light driven photocatalysis. Journal of Materials Science and Technology, 2021, 85, 1-10.	5.6	41
17	Promoted charge separation from nickel intervening in [Bi2O2]2+ layers of Bi2O2S crystals for enhanced photocatalytic CO2 conversion. Applied Catalysis B: Environmental, 2021, 294, 120249.	10.8	69
18	Photocatalytic N ₂ Reduction: Uncertainties in the Determination of Ammonia Production. ACS Sustainable Chemistry and Engineering, 2021, 9, 560-568.	3.2	20

Jun Li

#	Article	IF	CITATIONS
19	Boosting interfacial charge separation of Ba5Nb4O15/g-C3N4 photocatalysts by 2D/2D nanojunction towards efficient visible-light driven H2 generation. Applied Catalysis B: Environmental, 2020, 263, 117730.	10.8	168
20	Low boiling point solvent mediated strategy to synthesize functionalized monolayer carbon nitride for superior photocatalytic hydrogen evolution. Applied Catalysis B: Environmental, 2020, 260, 118181.	10.8	142
21	Ultrasonic-assisted fabrication of a direct Z-scheme BiOI/Bi2O4 heterojunction with superior visible light-responsive photocatalytic performance. Journal of Alloys and Compounds, 2020, 821, 153417.	2.8	59
22	Construction of 2D/2D Bi2Se3/g-C3N4 nanocomposite with High interfacial charge separation and photo-heat conversion efficiency for selective photocatalytic CO2 reduction. Applied Catalysis B: Environmental, 2020, 277, 119232.	10.8	140
23	Simultaneous reduction of Cr(VI) and degradation of tetracycline hydrochloride by a novel iron-modified rectorite composite through heterogeneous photo-Fenton processes. Chemical Engineering Journal, 2020, 393, 124758.	6.6	150
24	0D Bi nanodots/2D Bi3NbO7 nanosheets heterojunctions for efficient visible light photocatalytic degradation of antibiotics: Enhanced molecular oxygen activation and mechanism insight. Applied Catalysis B: Environmental, 2019, 240, 39-49.	10.8	218
25	Enhanced Generation of Reactive Oxygen Species under Visible Light Irradiation by Adjusting the Exposed Facet of FeWO ₄ Nanosheets To Activate Oxalic Acid for Organic Pollutant Removal and Cr(VI) Reduction. Environmental Science & Technology, 2019, 53, 11023-11030.	4.6	160
26	Ag-Bridged Z-Scheme 2D/2D Bi ₅ FeTi ₃ O ₁₅ /g-C ₃ N ₄ Heterojunction for Enhanced Photocatalysis: Mediator-Induced Interfacial Charge Transfer and Mechanism Insights. ACS Applied Materials & Interfaces, 2019, 11, 27686-27696.	4.0	200
27	One-Dimensional/Two-Dimensional Core–Shell-Structured Bi ₂ O ₄ /BiO _{2–<i>x</i>} Heterojunction for Highly Efficient Broad Spectrum Light-Driven Photocatalysis: Faster Interfacial Charge Transfer and Enhanced Molecular Oxvgen Activation Mechanism. ACS Applied Materials &: Interfaces. 2019. 11. 7112-7122.	4.0	111
28	Photocatalytic CO ₂ Conversion of M _{0.33} WO ₃ Directly from the Air with High Selectivity: Insight into Full Spectrum-Induced Reaction Mechanism. Journal of the American Chemical Society, 2019, 141, 5267-5274.	6.6	224
29	Full spectrum light driven photocatalytic in-situ epitaxy of one-unit-cell Bi2O2CO3 layers on Bi2O4 nanocrystals for highly efficient photocatalysis and mechanism unveiling. Applied Catalysis B: Environmental, 2019, 243, 667-677.	10.8	114
30	Ba ₅ Ta ₄ O ₁₅ Nanosheet/AgVO ₃ Nanoribbon Heterojunctions with Enhanced Photocatalytic Oxidation Performance: Hole Dominated Charge Transfer Path and Plasmonic Effect Insight. ACS Sustainable Chemistry and Engineering, 2018, 6, 6682-6692.	3.2	88
31	Enhanced molecular oxygen activation of Ni2+-doped BiO2-x nanosheets under UV, visible and near-infrared irradiation: Mechanism and DFT study. Applied Catalysis B: Environmental, 2018, 234, 167-177.	10.8	126
32	Z-scheme g-C3N4@CsxWO3 heterostructure as smart window coating for UV isolating, Vis penetrating, NIR shielding and full spectrum photocatalytic decomposing VOCs. Applied Catalysis B: Environmental, 2018, 229, 218-226.	10.8	164
33	Vacancyâ€Rich Monolayer BiO _{2â^<i>x</i>} as a Highly Efficient UV, Visible, and Nearâ€Infrared Responsive Photocatalyst. Angewandte Chemie - International Edition, 2018, 57, 491-495.	7.2	365
34	ZnO nanoparticles implanted in TiO2 macrochannels as an effective direct Z-scheme heterojunction photocatalyst for degradation of RhB. Applied Surface Science, 2018, 456, 666-675.	3.1	142
35	Noble metal-free modified ultrathin carbon nitride with promoted molecular oxygen activation for photocatalytic formaldehyde oxidization and DFT study. Applied Surface Science, 2018, 458, 59-69.	3.1	62
36	0D/2D Z-Scheme Heterojunctions of Bismuth Tantalate Quantum Dots/Ultrathin g-C ₃ N ₄ Nanosheets for Highly Efficient Visible Light Photocatalytic Degradation of Antibiotics. ACS Applied Materials & Interfaces, 2017, 9, 43704-43715.	4.0	313